



**HAL**  
open science

# Validated semi-analytical transition matrices for linearized relative spacecraft dynamics via Chebyshev series approximations

Paulo Ricardo Arantes Gilz, Florent Bréhard, Clément Gazzino

## ► To cite this version:

Paulo Ricardo Arantes Gilz, Florent Bréhard, Clément Gazzino. Validated semi-analytical transition matrices for linearized relative spacecraft dynamics via Chebyshev series approximations. 2018 Space Flight Mechanics Meeting, AIAA Science and Technology Forum and Exposition 2018, Jan 2018, Kissimmee, United States. 24p. hal-01540170v1

**HAL Id: hal-01540170**

**<https://hal.science/hal-01540170v1>**

Submitted on 15 Jun 2017 (v1), last revised 6 Feb 2018 (v3)

**HAL** is a multi-disciplinary open access archive for the deposit and dissemination of scientific research documents, whether they are published or not. The documents may come from teaching and research institutions in France or abroad, or from public or private research centers.

L'archive ouverte pluridisciplinaire **HAL**, est destinée au dépôt et à la diffusion de documents scientifiques de niveau recherche, publiés ou non, émanant des établissements d'enseignement et de recherche français ou étrangers, des laboratoires publics ou privés.

# Validated semi-analytical transition matrices for linearized relative spacecraft dynamics via Chebyshev series approximations

Paulo Ricardo Arantes Gilz\*      Florent Bréhard†  
Clément Gazzino ‡

## 1 Introduction

For spacecraft proximity operations (like rendezvous, station keeping, collision avoidance), the relative dynamics are often linearized for both propagation or control purposes. More specifically, when the magnitude of the relative motion of the spacecraft is small compared to its distance to the Earth, one linearizes the equations of motion, which implies solving simpler linear differential equations. However, no closed form solution is available for these equations in most cases. Exceptionally, for instance, Tschauner-Hempel equations for linearized Keplerian relative motion [33] admit an analytical solution for the transition matrix [35]. Other models, like the CNES Orange model [7] for geostationary orbit including moon and solar attraction, propose a semi-analytical approach where some coefficients of the differential equations are tabulated. A transition matrix is not available in this setting, except for the case when considering only the oblateness of the Earth, when some analytical methods were developed for the description of the relative motion [30, 14].

In the general case, the propagation is however performed with numerical iterative schemes (like Euler or Runge-Kutta). The main drawback of this discretization approach is that the number of needed evaluation points can be prohibitive and the discretization error is difficult to estimate precisely. Moreover, for control laws design purposes, analytical solutions are preferable, since various constraints (such as saturation, restricted space regions, etc.) can be satisfied on continuous time domains and not only on discretization grids.

On these lines, an interesting alternative is to obtain polynomial approximations of the solutions because they provide a more compact and accurate approximation and are easier to evaluate and manipulate. Recent works took advantage of such polynomial approximations in the context of model predictive control (MPC) and optimal impulsive constrained control [10, 1]. Their works follow the general framework of semidefinite programming (SDP) based on nonnegative polynomials written as sums of squares (SOS) [25].

---

\*LAAS, Université de Toulouse, CNRS, Toulouse, France prarante@laas.fr

†LIP, ENS Lyon, 46 Allée d'Italie, 69364 Lyon Cedex 07, France and LAAS-CNRS, 7 Avenue du Colonel Roche, 31077 Toulouse, France (florent.brehard@ens-lyon.fr).

‡LAAS, Université de Toulouse, CNRS, Toulouse, France cgazzino@laas.fr

The purpose of this article is to present a generic framework and algorithmic tool, which given the linearized equations of relative motion, provides a rigorous semi-analytical transition matrix, expressed as an approximating matrix whose entries are polynomials in Chebyshev basis, and uniform rigorous error bounds for each entry.

From the numerical point of view, spectral methods with Chebyshev expansions used in our work prove to be very efficient and accurate. Other recent works also highlight the advantage of using Chebyshev series expansions in orbital mechanics [28]. They started to successfully replace the classical Taylor series expansions based algebra for intrusive approaches, which has already many applications to astrodynamics and optimal control for proximity operations [21, 22, 11].

However, the scope of our work is not limited to numerical efficiency. The contribution of our algorithm is also to provide certified upper bounds for the approximation error (via a Newton-like *a posteriori* validation method), which allows to safely replace the exact solution with polynomials as long as the certified error bound remains smaller than a limit set by the user, depending on the application. This is particularly useful in optimization algorithms for optimal control where a trade-off must be done between low-degree polynomials for efficiency and accurate results.

The C source code of the whole method, including the efficient numerical algorithm for Chebyshev expansion of the solution and the automated validation process to certify these approximations, will be soon freely available<sup>1</sup>. Though still being under prototyping, it plainly works and was used for all the examples illustrating this article. Specifically, we chose two heterogeneous examples which allow us to highlight the generality of our approach: one handles the linearized relative motion of a satellite in Keplerian dynamics in low Earth orbit, the other focuses on linearizing relative dynamics in a geostationary orbit with applications to station keeping with a low-thrust propulsion system.

**Statement of the problem and contributions** In the light of the challenges mentioned above, the mathematical problem we want to solve can be stated as follows:

**Problem 1.** Consider a  $d$ -dimensional linear ordinary differential equation (LODE):

$$X'(t) = A(t)X(t) + D(t)$$

over the compact interval  $[t_0, t_f]$ , of unknown  $X : [t_0, t_f] \rightarrow \mathbb{R}^d$  and where  $A : [t_0, t_f] \rightarrow \mathbb{R}^{d \times d}$  and  $D : [t_0, t_f] \rightarrow \mathbb{R}^d$  are at least Lipschitz-continuous. Call  $\Phi(t_0, t)$  the exact mathematical transition matrix.

Provide an approximate transition matrix  $\tilde{\Phi}(t_0, t) \in \mathbb{R}^{d \times d}$  and rigorous error bounds  $\epsilon_{ij} \geq 0$  ( $1 \leq i, j \leq d$ ) satisfying:

$$|\tilde{\Phi}_{ij}(t_0, t) - \Phi_{ij}(t_0, t)| \leq \epsilon_{ij} \quad 1 \leq i, j \leq d, \quad t \in [t_0, t_f]$$

In Section 2, we present the whole method (numerical Chebyshev expansions and *a posteriori* validation) designed to automatically solve Problem 1. This method is fully exposed in [6], and Section 2 only sketches out the main

<sup>1</sup><http://perso.ens-lyon.fr/florent.brehard>

ingredients in order to give a precise idea of what was implemented, leaving out proofs and technical computations.

Section 3 is devoted to a first application of the method to Tschauner-Hempel equations, which are a rather easy case since dynamics can be decoupled between in-plane and out-of-plane motion and at the end reduced to scalar linear ordinary differential equations. We first show how the method will proceed on this example to output a rigorous semi-analytical transition matrix, though in practice this will be transparent to the user of our C library. Then, we explain where polynomial transition matrices can help for impulsive MPC, based on Nesterov generic framework. Finally, we perform an *a posteriori* validation to rigorously prove that the final position is reached within accurate precision.

Section 4 deals with another application: a linearized model for the station keeping of a geostationary satellite, taking into account the J2 perturbation term due to the oblateness of the Earth. In this case, the dynamical system cannot be easily decoupled into scalar differential equations. We will show that our method, generalized to the vectorial case, is able to provide certified and tight error bounds for each component of the motion. In a second time, the interest of having certified polynomial approximations of the transition matrix will be put into evidence.

## 2 Rigorous polynomial approximations of LODE solutions in Chebyshev basis

### 2.1 Chebyshev approximation theory and numerical solving

In many situations arising in scientific computing aimed at industrial applications, solving differential equations is a central building block. Since in most cases, obtaining exact closed forms for the solution is out of reach, a wide variety of numerical algorithms have been designed for decades to approximate these solutions as accurately as possible. In order to sketch out the picture, these methods can be divided into two groups:

- *Iterative methods* start at a given initial point with prescribed initial values, and propagate the solution on a time grid using explicit (Euler, explicit Runge-Kutta) or implicit (implicit Runge-Kutta) methods [18].
- On the opposite, *spectral methods* approximate the solution over the global time interval under consideration with a sum of well chosen basis functions, whose coefficients have to be computed [15, 5].

In situations where functions are smooth enough, spectral methods have the advantage over iterative ones of providing a smooth approximation of the solution over the continuous time range, which we can easily derive or integrate for example. For efficiency reasons among others, one often chooses families of polynomials for the basis functions, since addition and multiplication composing them are the basic operations implemented in floating-point units (FPU) of processors. Besides that, the recent advances in polynomial based optimization methods allowed for very efficient solutions in optimal control problems (see for instance [19, 8] and references therein). In this work, we focus on Chebyshev

polynomials, for this family of orthogonal polynomials enjoys very convenient algebraic and approximation properties.

**2.1.1 A short reminder on Chebyshev polynomials and approximation theory** At first glance, working with polynomials in the standard monomial basis and approximating functions with their Taylor development seems to be a convenient choice. In practice, this method goes along with some shortcomings (approximation of non-smooth functions, limited convergence radius due to complex singularities, numerical instability, etc.). For all these reasons, Chebyshev polynomials are preferable in the general case [5].

Here we briefly recall the main properties of Chebyshev polynomials. This family of polynomials is defined by the three-term recurrence  $T_{n+2} = 2XT_{n+1} - T_n$  with initial terms  $T_0 = 1$  and  $T_1 = X$ . They satisfy the fundamental trigonometric relation  $T_n(\cos \vartheta) = \cos(n\vartheta)$ , from which we deduce some of their basic algebraic properties:

$$T_n T_m = \frac{1}{2}(T_{n+m} + T_{|n-m|}) \quad \left[ \frac{T_{n+1}}{2(n+1)} - \frac{T_{n-1}}{2(n-1)} \right]' = T_n \quad (n \geq 2)$$

and that  $|T_n(t)| \leq 1$  for  $x \in [-1, 1]$ .

Endowing the space  $\mathcal{C}^0$  of continuous functions over the compact interval  $[-1, 1]$  with a Hilbert space structure using the inner product defined by  $\langle f, g \rangle = \int_{-1}^1 f(t)g(t)(1-t^2)^{-1/2}dt = \int_0^\pi f(\cos \vartheta)g(\cos \vartheta)d\vartheta$ , we see the Chebyshev polynomials as an orthogonal family. To any continuous function  $f$  we can associate its Chebyshev coefficients:

$$[f]_0 = \frac{1}{\pi} \int_0^\pi f(\cos \vartheta)d\vartheta \quad [f]_n = \frac{2}{\pi} \int_0^\pi f(\cos \vartheta) \cos(n\vartheta)d\vartheta \quad (n \geq 1)$$

Hence, the truncated Chebyshev series  $f^{[n]} = \sum_{i=0}^n [f]_i T_i$  of  $f$  is simply the orthogonal projection of  $f$  onto the finite-dimensional subspace spanned by  $T_0, \dots, T_n$ . Analogously to Fourier series, Chebyshev series enjoy excellent approximation properties [5]. For example, if  $f$  is of class  $\mathcal{C}^r$  over  $[-1, 1]$  with  $r \geq 1$ , then  $f^{[n]}$  uniformly converges to  $f$  in  $O(n^{-r})$ . Moreover, at fixed degree  $n$ , the  $n$ -th truncated Chebyshev series  $f^{[n]}$  is a near-best approximation of  $f$  among degree  $n$  polynomials, with a factor growing relatively slowly, in  $O(\log(n))$  [24].

Using these convergence results, one can easily identify a sufficiently smooth function space with the space of corresponding Chebyshev coefficients. Let's call  $\mathfrak{V}^1$  the Banach space of continuous functions with absolutely summable Chebyshev series, and define the associated norm  $\|f\|_{\mathfrak{V}^1} = \sum_{i \geq 0} |[f]_i|$ . We obtain a Banach algebra structure, for we have  $\|fg\|_{\mathfrak{V}^1} \leq \|f\|_{\mathfrak{V}^1} \|g\|_{\mathfrak{V}^1}$ . Moreover, this norm is a safe overestimation of the supremum norm  $\|\cdot\|_\infty$  over  $[-1, 1]$ :

$$\|f\|_{\mathfrak{V}^1} = \sum_{i \geq 0} |[f]_i| \geq \sup_{-1 \leq t \leq 1} \sum_{i \geq 0} |[f]_i T_i(t)| \geq \sup_{-1 \leq t \leq 1} |f(t)| = \|f\|_\infty$$

**2.1.2 Integral transform, almost-banded structure and efficient numerical solving algorithm** In this article, we consider Linear Ordinary Differential Equations (LODE) of the form:

$$y^{(r)}(t) + a_{r-1}(t)y^{(r-1)}(t) + \dots + a_1(t)y'(t) + a_0(t)y(t) = g(t) \quad (1)$$

together with prescribed initial values at  $-1$ :

$$y(-1) = v_0 \quad y'(-1) = v_1 \quad \dots \quad y^{(r-1)}(-1) = v_{r-1} \quad (2)$$

where  $a_i, g : [-1, -1] \rightarrow \mathbb{R}$  are functions in  $\mathcal{C}^1$  approximated by a truncated Chebyshev series, and  $y : [-1, 1] \rightarrow \mathbb{R}$  is the unknown function which we want to approximate with a truncated Chebyshev series. For this, a common solution is to rephrase the differential equation (1) into an equivalent integral equation. For instance, as detailed in [6], one considers  $\varphi = y^{(r)}$  as the unknown function and expresses lower-order derivatives of  $y$  as integrals of  $\varphi$ . This gives:

$$\varphi + \mathbf{K} \cdot \varphi = \psi \quad \text{where} \quad \mathbf{K} \cdot \varphi(t) = \int_{-1}^t k(t, s) \varphi(s) ds \quad (3)$$

with  $k(t, s)$  a bivariate polynomial easily computed from the polynomials  $a_i(t)$ . A symbolic computation shows that for  $i \in \mathbb{N}$ ,  $\mathbf{K} \cdot T_i$  is a polynomial with non-zero Chebyshev coefficients between indices 0 and  $h$  (initial coefficients) and between  $i - d$  and  $i + d$  (diagonal coefficients), where the bandwidths  $h$  and  $d$  directly depend on the maximum degree of the  $a_i$ . Hence, the operator  $\mathbf{K} : \mathcal{C}^1 \rightarrow \mathcal{C}^1$  has a so-called almost-banded structure [26, 6] in the Chebyshev basis, which is depicted on Figure 1.

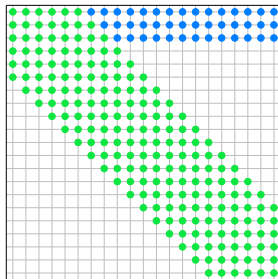


**Figure 1:** Matrix representation of  $\mathbf{K}$  in Chebyshev basis, truncated at order 20. Almost-banded structure given by initial coefficients (blue) and diagonal ones (green)

Following the general scheme of spectral Galerkin methods [5], we project this problem into finite dimension by taking the truncated operator  $\mathbf{K}^{[n]} = \pi_n \cdot \mathbf{K} \cdot \pi_n$  where  $\pi_n$  is the orthogonal projection from  $\mathcal{C}^1$  to the finite-dimensional space spanned by  $T_0, \dots, T_n$ . Now, it remains to determine the  $n + 1$  first (approximated) Chebyshev coefficients of  $\varphi$  by solving the following finite-dimensional problem:

$$\varphi + \mathbf{K}^{[n]} \cdot \varphi = \psi$$

Such an almost-banded system is efficiently solved using the algorithm presented in [26]. The mathematical statements and proofs establishing the uniqueness of the solution and the exponential convergence of the numerical truncated solutions to the exact one are to be found in [6].

As a final remark, we note that this method can be extended to the vectorial case, where  $y, g : [-1, 1] \rightarrow \mathbb{R}^p$  and  $a_i : [-1, 1] \rightarrow \mathbb{R}^{p \times p}$ . To see this, first notice that the integral transform can be applied as in the scalar case described above. The resulting operator  $\mathbf{K} : (\mathcal{C}^1)^p \rightarrow (\mathcal{C}^1)^p$  is made of

$p \times p$  (scalar) integral operators  $\mathbf{K}_{ij} : \mathcal{U}^1 \rightarrow \mathcal{U}^1$  as above (see Figure 2(a)). By rearranging the basis of  $(\mathcal{U}^1)^p$  from  $T_{0,1}, T_{1,1}, T_{2,1}, \dots, T_{0,p}, T_{1,p}, T_{2,p}, \dots$  to  $T_{0,1}, \dots, T_{0,p}, T_{1,1}, \dots, T_{1,p}, \dots$ , where  $T_{i,j}$  designates the  $i$ -th Chebyshev polynomial in the  $j$ -th component of  $\mathbb{R}^p$ , we end up again with an almost-banded structure depicted in Figure 2(b). Hence, the numerical solving essentially works as in the scalar case.

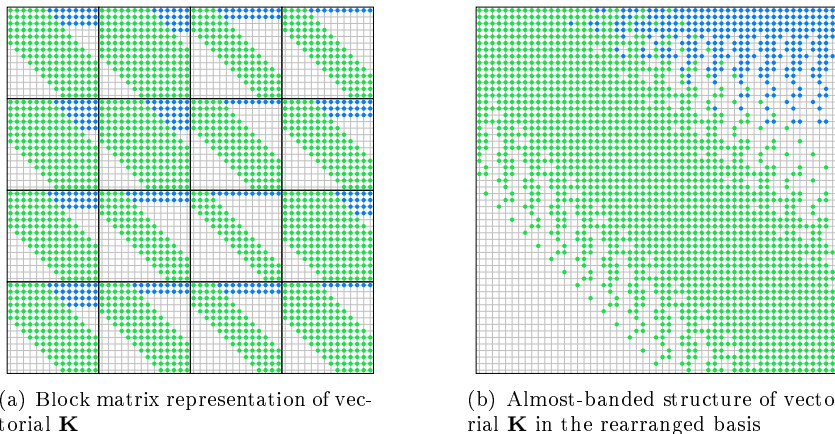


**Figure 2:** Two representations of vectorial integral operator  $\mathbf{K}$

## 2.2 Validation method

Most of numerical solving methods for differential equations are justified by convergence theorems, estimating how fast the numerical approximations tend to the exact solution when some parameter (number of discretization points, degree of approximating polynomials, etc.) tends to infinity. However, it often appears that these estimates involve non-effective upper bounds (like a bound on the  $k$ -th derivative of the solution). Moreover, they do not take into account the inherent rounding errors of floating-point arithmetics. For all these reasons, such convergence results just state that *asymptotically* and for a *sufficiently large* floating-point precision, the solving method is well behaved, but nothing can be said about a particular solution obtained with finite parameters and precision.

The goal of validating techniques is to provide such effective and rigorous error bounds for given approximations. Two main families with different approaches may be distinguished:

- *Self-validating methods* construct an approximation together with a rigorous error bound at one time. In the context of differential equations, they are often combined with iterative methods, bounding at each step the error committed at the current discretization point and propagating it for the following ones.
- *A posteriori validation methods* work in two times. First, the user provides an approximation of the solution, obtained with the procedure of his choice. Then, the validation method computes a rigorous error bound without knowing how this approximation was built.

The paradigm of *a posteriori* validation methods is particularly well suited for spectral methods. Since we explained in the previous section how to compute approximate solutions for LODE (1), we can now suppose that some approximating truncated Chebyshev series is given and focus on the validation method itself.

**2.2.1 General ideas for designing a *a posteriori* validation methods** A wide majority of *a posteriori* validation methods are based on Banach fixed-point theorem and variations around it. Since this article only tackles linear problems, this theorem can be stated in this simplified version:

**Theorem 1.** *Let  $(E, \|\cdot\|_E)$  be a Banach space and  $\mathbf{T} : E \rightarrow E$  an affine operator whose linear part  $\mathcal{D}\mathbf{T}$  is a bounded linear endomorphism. If  $\mathbf{T}$  is contracting, that is, if  $\|\mathcal{D}\mathbf{T}\|_E = \mu < 1$ , then it admits a (necessarily unique) fixed point  $x^* \in E$ , solution of the equation:*

$$\mathbf{T} \cdot x = x \tag{4}$$

and for a given  $\tilde{x} \in E$ , we have the following enclosure for its distance to  $x^*$ :

$$\frac{\|\tilde{x} - \mathbf{T} \cdot \tilde{x}\|_E}{1 + \mu} \leq \|\tilde{x} - x^*\|_E \leq \frac{\|\tilde{x} - \mathbf{T} \cdot \tilde{x}\|_E}{1 - \mu} \tag{5}$$

Hence, designing a fixed-point based validation method for a linear problem of the form  $\mathbf{F} \cdot x = y$  essentially boils down to rephrasing it as a fixed-point equation  $\mathbf{T} \cdot x = x$  for some contracting affine operator  $\mathbf{T}$ , which has to be explicitly computable (in order to bound  $\|\tilde{x} - \mathbf{T} \cdot \tilde{x}\|_E$ ) and whose operator norm can be effectively upper-bounded so to obtain a rigorous  $\mu < 1$ .

A rather generic way to design such a contracting method is to use an adaptation of Newton's method to find zeros of maps [34], which can be used even for non-linear problems. Here we sketch the idea in the linear case. Consider the equation  $\mathbf{F} \cdot x = y$ , where  $\mathbf{F}$  is a linear automorphism. Let  $\mathbf{A}$  be an approximation of its inverse  $\mathbf{F}^{-1}$ . Then the unique solution is also the unique fixed-point of  $\mathbf{T}$  defined by:

$$\mathbf{T} \cdot x = x - \mathbf{A} \cdot (\mathbf{F} \cdot x - y) \tag{6}$$

as soon as  $\mathbf{A}$  is injective. The underlying idea is that if  $\mathbf{A}$  is sufficiently close to the inverse of  $\mathbf{F}$ , then  $\mathbf{T}$  will be contracting.

The remaining work then consists in finding an appropriate  $\mathbf{A}$  and bounding the linear part of the resulting  $\mathbf{T}$ . Such techniques are widely advocated in, for example [34], but quite often, technical tools to design such a Newton operator are treated by hand for precise examples. On the contrary, the method we present below is fully algorithmic over the general case of LODEs and implemented into a C library.

**2.2.2 Principles of our validation method** Applying variations of Newton's methods to ODEs, even non-linear ones, is not a new idea *per se* (see for examples instructive works [20]). Our method however aims at providing a generic, fully automated and rather efficient algorithm, which could be used as part of a library for rigorous computing as a black box from the point of view of the user.

Considering again the integral reformulation (3) of the problem, we choose a truncation index  $n$  and seek an approximate inverse  $\mathbf{A}$  of  $\mathbf{I} + \mathbf{K}$  as an approximation of the finite-dimensional truncated operator  $\mathbf{I} + \mathbf{K}^{[n]}$ . Unfortunately, the inverse of this  $n + 1$  order almost-banded square matrix is dense in general. However, we discuss in [6] the possibility to approximate this inverse with an almost-banded matrix itself.

Having this  $\mathbf{A}$  fully determines our Newton-like affine operator  $\mathbf{T} : \varphi \mapsto \varphi - \mathbf{A} \cdot (\varphi + \mathbf{K} \cdot \varphi - \psi)$ . Its linear part  $\mathbf{I} - \mathbf{A} \cdot (\mathbf{I} + \mathbf{K})$  may be bound using the following decomposition of its operator norm:

$$\|\mathbf{I} - \mathbf{A} \cdot (\mathbf{I} + \mathbf{K})\|_{\mathcal{U}^1} \leq \|\mathbf{I} - \mathbf{A} \cdot (\mathbf{I} + \mathbf{K}^{[n]})\|_{\mathcal{U}^1} + \|\mathbf{A} \cdot (\mathbf{K} - \mathbf{K}^{[n]})\|_{\mathcal{U}^1} \quad (7)$$

- The first term is the approximation error, since  $\mathbf{A}$  is only an approximation of  $(\mathbf{I} + \mathbf{K}^{[n]})^{-1}$ . It boils down to the computation of an  $n + 1$  order square matrix using multiplications and additions, which is carried out using interval arithmetics to avoid rounding errors.
- The second part is the truncation error, due to the fact that  $\mathbf{K}^{[n]}$  is only a finite-dimensional approximation of  $\mathbf{K}$ .

The difficulty really lies in this second error term, obtained by uniformly bounding  $\|\mathbf{A} \cdot (\mathbf{K} - \mathbf{K}^{[n]}) \cdot T_i\|_{\mathcal{U}^1}$  with respect to  $i$ . A good bounding strategy should avoid huge overestimations, for it would lead the method to choose far larger values of  $n$  than needed to obtain a contracting  $\mathbf{T}$ . We refer to [6] for a detailed exposure of an efficient technique we use for this purpose.

An extended discussion on the smallest value of  $n$  this validation method allows to choose for the Newton-like operator  $\mathbf{T}$  to be contracting and on the overall complexity of the algorithm is engaged in [6]. The conclusion is that this  $n$  suffers an exponential bound with respect to the magnitude of the Chebyshev coefficients of the  $a_i$ , but that in practice, for a wide range of reasonable examples, this method is quite efficient and fully automated.

**2.2.3 Extensions of the method** Several extensions of the method are considered to treat a larger variety of LODEs:

- In many problems arising in physics, including the spacecraft dynamics studied in this article, the coefficients and right hand side in LODE (1) are not polynomials (rational functions, special functions, etc.). If they belong to  $\mathcal{U}^1$  and are given through truncated Chebyshev series with a certified error bound with respect to the  $\mathcal{U}^1$ -norm, then the exact integral operator  $\mathbf{K}$  is non-polynomial but well approximated by the polynomial integral operator  $\mathbf{K}_P$  obtained by replacing the true coefficients by their polynomial approximations. An additional term  $\|\mathbf{A} \cdot (\mathbf{K} - \mathbf{K}_P)\|_{\mathcal{U}^1}$  appends to the two others in (7), but the essential ideas of the method remain unchanged.
- Since we deal with linear problems only in this article, generalized boundary value problems (BVP) can be rigorously solved by computing a basis of certified solutions. Though, we would like in the future to find an *ad-hoc* method for such problems, since working with a basis of solutions and recombine them could lead to worse conditioned numerical solutions and overestimated error bounds.

- Our validation method can also be generalized to the vectorial case. The ongoing work of one of the authors aims to extend the framework of fixed-point based validation to the vectorial case with individual tight error bounds for each component of the solution to be validated. In the particular case of LODE validation, the tools involved in the one-dimensional case are easily transposed to the vectorial case. This work is still not published, but an implementation of the vectorial case is also included in the C library and used in Section 4.

### 3 Linearized impulsive rendezvous using Tschauner and Hempel equations and embedded model predictive control

As a first example to our method presented in Section 2, we consider the linearized relative motion of a satellite in Keplerian dynamics. In a moving Local-Vertical-Local-Horizontal (LVLH) frame located at the target's position, let  $x$ ,  $y$  and  $z$  denote the relative position of the chaser along respectively the in-track, cross-track and radial axes. In [33], Tschauner and Hempel show that by a suitable change of independent variable from the time  $t$  to the true anomaly  $\nu$  and by working with rescaled coordinates  $(\tilde{x}, \tilde{y}, \tilde{z})^T = (1 + e \cos \nu)(x, y, z)^T$ , we obtain the following linearized equations:

$$\tilde{x}''(\nu) = 2\tilde{z}'(\nu) \quad (8)$$

$$\tilde{y}''(\nu) = -\tilde{y}(\nu) \quad (9)$$

$$\tilde{z}''(\nu) = \frac{3}{1 + e \cos \nu} \tilde{z}(\nu) - 2\tilde{x}'(\nu) \quad (10)$$

We observe that the in-plane motion ( $\tilde{x}$  and  $\tilde{z}$ ) is decoupled from the out-of-plane motion ( $\tilde{y}$ ). The latter involves only one coordinate and is a simple harmonic oscillator. The former involves two coordinates, but  $\tilde{x}'$  can be easily eliminated from the equation of  $\tilde{z}$ , which becomes:

$$\tilde{z}''(\nu) + \left(4 - \frac{3}{1 + e \cos \nu}\right) \tilde{z}(\nu) = c \quad (11)$$

where the constant  $c$  is defined from the initial conditions:

$$c = 4\tilde{z}(\nu_0) - 2\tilde{x}'(\nu_0) \quad (12)$$

First, we analyze precisely in Section 3.1 how the method will work on this example in order to produce an approximating Chebyshev expansion of the trajectory and a rigorous error bound. This is done for pedagogical reasons, but in practice the approximation and validation algorithms in the C library run as a black box from the point of view of the user.

Then, in Section 3.2, we briefly present the work of one of the author about a predictive control algorithm for spacecraft rendezvous [1]. The underlying polynomial optimization problem justifies the need for low-degree but still accurate polynomial approximations of the transition matrix.

Finally in Section 3.3, we use the power of the validation method to perform an *a posteriori* verification of an instance of rendezvous by providing a rigorous

enclosure of the chaser's final position. This is particularly important for safety critical missions.

### 3.1 Rigorous semi-analytical transition matrix for Tschauner-Hempel equations

Before running the method on LODE 11, we first rescale the interval  $[\nu_0, \nu_f]$  to  $[-1, 1]$  by introducing the independent variable  $\tau \in [-1, 1]$  and letting  $\nu(\tau) = \nu_0(1 - \tau)/2 + \nu_f(1 + \tau)/2 = \omega\tau + \theta$  with  $\omega = (\nu_f - \nu_0)/2$  and  $\theta = (\nu_0 + \nu_f)/2$ , and  $Z(\tau) = z(\nu(\tau))$ . We obtain:

$$Z''(\tau) + \omega^2 \left( 4 - \frac{3}{1 + e \cos \nu(\tau)} \right) Z(\tau) = \omega^2 c \quad (13)$$

together with rescaled initial conditions:

$$Z(-1) = z(\nu_0) \quad Z'(-1) = \omega z'(\nu_0)$$

In particular, we observe that the magnitude of the coefficients in Equation (13) grows quadratically with the length of the interval  $[\nu_0, \nu_f]$  over which we want to approximate the trajectory.

**3.1.1 Rigorous approximation of the coefficient** The first obstacle we must face is that the coefficient of Equation (13) is not polynomial because of the function  $\tau \mapsto (1 + e \cos \nu(\tau))^{-1}$ . Hence, our first task is to provide a rigorous polynomial approximation for it.

The cosine function  $\tau \mapsto \cos \nu(\tau)$  is approximated by applying our validation method to the harmonic oscillator differential equation:

$$y''(\tau) + \omega^2 y(\tau) = 0 \quad y(-1) = \cos \nu_0 \quad y'(-1) = -\omega \sin \nu_0$$

From this, we deduce a rigorous approximation of  $\tau \mapsto 1 + e \cos \nu(\tau)$ .

Finally, it must be composed with the reciprocal function. Numerical approximations can be obtained using interpolation at Chebyshev nodes, which is a very standard and rather efficient method [5]. Validation is performed through another Newton-like fixed-point method. Without entering to deeply into details, we sketch out the principle. Let  $f$  be a function in  $\mathcal{Q}^1$ , non-zero over  $[-1, 1]$ , to be inverted, and  $g = 1/f$  the solution function. We must solve the functional equation  $fg - 1 = 0$  of unknown  $g \in \mathcal{Q}^1$  (the fact that  $g = 1/f$  belongs to  $\mathcal{Q}^1$  comes from Wiener's Tauberian theorem). If  $g_0$  is a polynomial approximation of  $g$  satisfying  $\|1 - g_0 f\|_{\mathcal{Q}^1} = \mu < 1$ , then  $g$  is the unique fixed-point of the affine operator  $\mathbf{T}$  defined by  $\mathbf{T} \cdot g = g - g_0(fg - 1)$  and of Lipschitz constant  $\mu < 1$ . Hence, Theorem 1 applies and provides an error enclosure for any candidate approximation  $\tilde{g}$  of  $g$ .

Figure 3(a) shows the evolution of the minimal degree  $p$  needed to approximate the coefficient  $\tau \mapsto \omega^2(4 - 3/(1 + e \cos \nu(\tau)))$  within a  $\mathcal{Q}^1$ -error less than 1, in function of the eccentricity  $e$  and the total time interval  $[\nu_0, \nu_f]$ .

**3.1.2 Integral transform and numerical solving** Following the integral transform technique described above, we let  $\varphi(\tau) = Z''(\tau)$ , so that  $Z(\tau)$  now

becomes:

$$\begin{aligned} Z(\tau) &= Z(-1) + (\tau + 1)Z'(-1) + \int_{-1}^{\tau} \int_{-1}^s \varphi(u) du \\ &= Z(-1) + (\tau + 1)Z'(-1) + \int_{-1}^{\tau} (\tau - s)\varphi(s) ds \end{aligned}$$

We thus obtain the integral equation:

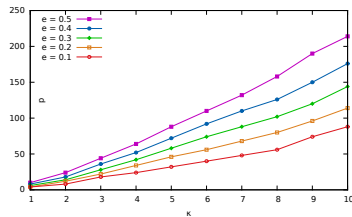
$$\varphi(\tau) + \int_{-1}^{\tau} \alpha(\tau)(\tau - s)\varphi(s) ds = \omega^2 c - \alpha(\tau)(Z(-1) + (\tau + 1)Z'(-1))$$

where  $\alpha(\tau) = 4 - 3/(1 + e \cos \nu(\tau))$ .

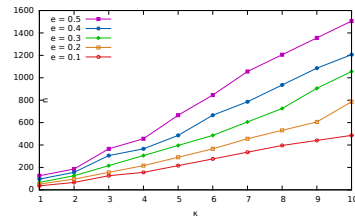
For the numerical solving, replace  $\alpha(\tau)$  by a polynomial approximation  $a(\tau)$  and proceed as in 2.1.2: truncate resulting infinite-dimensional equations at a chosen index  $n$  and solve the resulting almost-banded system using the algorithm presented in [26] to obtain a polynomial approximation of degree  $n$  of the solution.

**3.1.3 Validation** The validation method we presented in Section 2.2 is fully automated. Hence, in this practical example, it just suffices to provide to the implemented procedure the differential equation (13) where  $\alpha(\tau)$  is given as a polynomial approximation  $a(\tau)$  together with the error bound  $\varepsilon$ , and the candidate polynomial approximate solution  $\tilde{\varphi}$  obtained just above. The procedure will return a rigorous upper bound of the approximation error, with respect to the  $\Psi^1$ -norm.

However, the timings strongly depend on the minimal value for the truncation index the method will be able to find in order to ensure that the obtained operator is contracting. Figure 3(b) gives these values in function of the time interval  $\nu_f - \nu_0$  and the eccentricity  $e$  of the target reference orbit. We stress out the fact that these values only depend on the equation (that is,  $\nu_0$ ,  $\nu_f$  and  $e$ ) and not on the degree of the candidate approximate solution  $\tilde{\varphi}$ , since the contracting operator  $\mathbf{T}$  is completely independent of this approximation and just need to be contracting.



(a) Approximation degree  $p$  needed to approximate coefficient  $\tau \mapsto \omega^2(4 - 3/(1 + e \cos \nu(\tau)))$  with a  $\Psi^1$ -error less than 1



(b) Truncation order  $n$  needed to obtain a contracting Newton-like operator for LODE (13)

**Figure 3:** Parameters evolution during validation of LODE (13) in function of eccentricity  $e$  and total time  $[\nu_0, \nu_f] = [0, 2\kappa\pi]$

The results exposed in Figure 3(b) show that a straightforward application of the validation method tends to rapidly become time-consuming after about 10 periods. In next section, we explain how to exploit the periodicity of the equation to validate a freely propagated trajectory over a large number of periods.

**3.1.4 Long-term validated integration techniques** Since Equation (11) is  $2\pi$ -periodic, validating a transition matrix over  $[\nu_0, \nu_0 + 2\pi]$  is a good starting point for most applications:

$$\tilde{\Phi}(\nu_0, \nu) = \begin{pmatrix} \tilde{x}_{(i)}(\nu) & \tilde{x}_{(ii)}(\nu) & \tilde{x}_{(iii)}(\nu) & \tilde{x}_{(iv)}(\nu) \\ \tilde{z}_{(i)}(\nu) & \tilde{z}_{(ii)}(\nu) & \tilde{z}_{(iii)}(\nu) & \tilde{z}_{(iv)}(\nu) \\ \tilde{x}'_{(i)}(\nu) & \tilde{x}'_{(ii)}(\nu) & \tilde{x}'_{(iii)}(\nu) & \tilde{x}'_{(iv)}(\nu) \\ \tilde{z}'_{(i)}(\nu) & \tilde{z}'_{(ii)}(\nu) & \tilde{z}'_{(iii)}(\nu) & \tilde{z}'_{(iv)}(\nu) \end{pmatrix}$$

Column of index  $(i)$ , (resp.  $(ii)$ ,  $(iii)$  and  $(iv)$ ) is a certified approximation of the in-plane trajectory corresponding to the initial conditions  $\tilde{x}(\nu_0) = 1$  (resp.  $\tilde{z}(\nu_0) = 1$ ,  $\tilde{x}'(\nu_0) = 1$  and  $\tilde{z}'(\nu_0) = 1$ ), all the other initial values being set to 0.

To ensure validated propagation over several periods, two different approaches may be considered:

- This transition matrix can be used to provide a separate polynomial approximation over each period  $[\nu_0 + 2k\pi, \nu_0 + 2(k+1)\pi]$ . Call  $J = \tilde{\Phi}(\nu_0, \nu_0 + 2\pi)$  the matrix of rigorous enclosures of the final states after one period. The trajectory over period  $[\nu_0 + 2k\pi, \nu_0 + 2(k+1)\pi]$  is rigorously approximated by:

$$\begin{pmatrix} \tilde{x}(\nu) \\ \tilde{z}(\nu) \\ \tilde{x}'(\nu) \\ \tilde{z}'(\nu) \end{pmatrix} \in \tilde{\Phi}(\nu_0, \nu - 2k\pi) J^k \begin{pmatrix} \tilde{x}(\nu_0) \\ \tilde{z}(\nu_0) \\ \tilde{x}'(\nu_0) \\ \tilde{z}'(\nu_0) \end{pmatrix} \quad (14)$$

Several remarks should be made. First, this method does not provide a uniform rigorous polynomial approximation over the whole time interval under consideration. Then, if the entries of  $J$  are rather loose intervals, which arises when  $\tilde{\Phi}(\nu_0, \cdot)$  is made of low-degree polynomial approximations, then the intervals in  $J^k$  will rapidly become very large and all precision will be lost after a certain number of periods.

- In some situations however, we absolutely need a uniform polynomial approximation over the whole time interval. Following Section 3.1.2, we obtain a polynomial approximation for the trajectory  $X(\nu) = (\tilde{x}(\nu), \tilde{z}(\nu), \tilde{x}'(\nu), \tilde{z}'(\nu))$  over  $[\nu_0, \nu_f]$  where  $\nu_f = \nu_0 + 2\kappa\pi$ . To perform an *a posteriori* validation, let's suppose that we have a tight enough transition matrix  $\tilde{\Phi}(\nu_0, \cdot)$ , so that we can recover a very precise piecewise polynomial approximation (14). The final task is to bound the difference over each period  $[\nu_0 + 2k\pi, \nu_0 + 2(k+1)\pi]$  ( $0 \leq k < \kappa$ ) between this very precise approximation and the candidate approximation  $X(\nu)$  restricted over this period. Remember however that all approximations are truncated Chebyshev series over  $[-1, 1]$  representing rescaled functions so that their definition interval is  $[-1, 1]$ . Hence, for each period,  $X$  must be composed on the right

by an affine time rescaling so to extract the desired time subinterval and compare the resulting Chebyshev truncated series with the corresponding precise approximation. Bounding this difference using the  $\Psi^1$ -norm and adding to it the rigorous error bound of the precise solution gives a safe overestimation of the uniform error.

### 3.2 Embedded model predictive control using the certified polynomial transition matrices

The spacecraft rendezvous model with Tschauner-Hempel equations (8) can be employed in the design and control of satellite trajectories. One of the applications of interest is the conception of MPC (model predictive control) for automatically on-line computing the maneuvers for guiding the satellites to the desired constrained trajectories (see [16]).

The method for obtaining rigorous polynomial approximations of the transition matrices presented in Section 2 is particularly well-suited for this purpose because, since it is based on Chebyshev polynomials, the constraints and the criterion to be optimized can be addressed by the parametrization of non-negative polynomials on the cone of positive semidefinite matrices (see [25, 10, 2]).

In the sequel, we present the state propagation for the impulsive rendezvous and the constraints related to this problem to lastly formulate the MPC optimization problem.

#### 3.2.1 Model predictive control intermediary problems formulation

Let be a  $d$ -dimensional linear time-variant dynamical system:

$$\dot{X} = A(t)X + B(t)u \quad (15)$$

where in our case  $A$  is the matrix corresponding to Tschauner-Hempel equations (8) (but could be an arbitrary linear model), for which the evolution of the state can be represented by  $\tilde{\Phi}$ , a rigorous polynomial approximation of its transition matrix, as follows:

$$X(t_N) = \tilde{\Phi}(t_1, t_N)X(t_1) + \int_{t_1}^{t_N} \tilde{\Phi}(s, t_N)B(s)u(s)ds, \quad (16)$$

where the vector  $u$  is the control and  $t_1$  and  $t_N$  are respectively the initial and final time of propagation of the state. In the case of impulsive spacecraft rendezvous problems, the control thrusts are modeled as Dirac deltas, which results in the following space-transition:

$$X(t_N) = \tilde{\Phi}(t_1, t_N)X(t_1) + \sum_{i=1}^N \tilde{\Phi}(t_i, t_N)B(t_i)u(t_i), \quad (17)$$

where the vectors  $u_i$  (the decision variables) represent the impulsive velocity corrections applied at instants  $t_i$  and  $N$  is the number of impulses applied in order to bring the satellite to the desired trajectory.

For proximity operations, the relative motion between spacecraft must respect affine constraints, such as visibility cones, safety boundaries, hovering zones, etc. These constraints are modeled as follows:

$$\underline{X} \leq H X(t) \leq \overline{X}, \quad t_j \leq t \leq t_{j+1}, \quad j = 1, \dots, N-1 \quad (18)$$

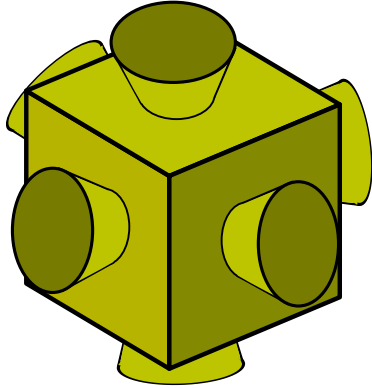
where  $H \in \mathbb{R}^{k \times d}$  is a constant matrix and  $\underline{X}, \bar{X} \in \mathbb{R}^k$  are the bounds.

The dead-zone and saturation constraints for the actuators can be taken into account by the following inequalities:

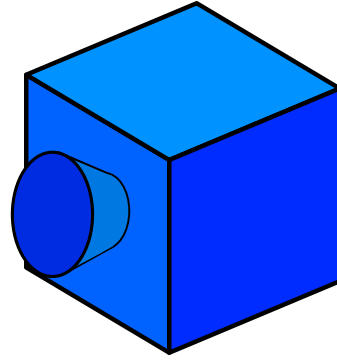
$$\underline{u}_i \leq u(t_i) \leq \bar{u}_i, \quad i = 1, \dots, N \quad (19)$$

The criterion to be minimized is the fuel-consumption, which is modeled by the  $\ell_1$ -norm or the  $\ell_2$ -norm of the thrusts depending on the configuration of the actuators (see Fig. 4 and [29] for details):

$$\text{Objective: } \min_u \sum_{i=1}^N \|u_i\|_p, \quad p = 1 \text{ or } 2 \quad (20)$$



(a) Spacecraft controlled by three pairs of axially symmetrically disposed thrusters:  $p = 1$ .



(b) Spacecraft controlled by one single thruster by gimbaling:  $p = 2$ .

**Figure 4:** Two possible configurations for the spacecraft thrusters.

The MPC strategy supposes that we have some *a priori* knowledge on the behavior of the studied system (in our case, the state-transition). A criterion to be minimized is formulated in function of the consumption related to the maneuvers that must be applied to steer the spacecrafts to a trajectory respecting the imposed constraints and also in function of the predicted trajectory. This criterion is then iteratively optimized (different types of horizons can be adopted, see [27] for details) and the consecutive application of the computed control actions is supposed to steer the dynamical system to the desired trajectory.

Independently of the type of horizon strategy used, each instance of the MPC optimization problem can be formulated via the relations (17), (18), (19) and (20):

$$\begin{aligned} \min_u \quad & \sum_{i=1}^N \|u_i\|_p, \quad p = 1 \text{ or } 2 \\ \text{s.t.} \quad & \begin{cases} X(t_N) = \tilde{\Phi}(t_1, t_N)X(t_1) + \sum_{i=1}^N \tilde{\Phi}(t_i, t_N)B(t_i)u(t_i) \\ \underline{X} \leq H X(t) \leq \bar{X}, \quad t_j \leq t \leq t_{j+1}, \quad j = 1, \dots, N-1 \\ \underline{u}_i \leq u(t_i) \leq \bar{u}_i, \quad i = 1, \dots, N \end{cases} \end{aligned} \quad (21)$$

**3.2.2 Ongoing work and comparison with existing technique** Our ongoing work consists in computing certified semi-analytical polynomial transition matrices  $\tilde{\Phi}(t_i, \cdot)$  of reasonable degree, in order to plug them into the optimization problem (21) and solve it. In fact, since the certified propagated state  $X(t)$  is described by polynomials, the affine constraints can be rewritten as polynomial non-negativity constraints. Using the parametrization of non-negative polynomials on the cone of semidefinite positive matrices [25], the optimization problem can then be reformulated into a SDP program. This type of optimization problem has already been addressed in previous works on spacecraft rendezvous [10, 1]. Particularly in the latter reference, a MPC algorithm based on small SDP programs was tested on a device dedicated to space applications (a AEROFLEX GAISLER GR-XC6S board containing a synthesized LEON3 microprocessor), showing good performances. Analogously, future experiments would assess the on-board tractability of the SDP version of (21), focusing on the analysis of the relation between the computational burden and the precision of the polynomial approximations.

### 3.3 Validated Rendezvous

In open loop impulsive rendezvous problems, optimization algorithms like the one described above to solve (21) determine the locations and values of the impulses to apply in order to reach the prescribed final position while minimizing the total fuel consumption. In this section, we suppose given these impulses. Our goal is to certify the final position of the chaser, assuming linearized Keplerian dynamics.

Having at hand algorithmic tools for certified trajectory propagation (Sections 3.1.3 and 3.1.4), the principle for certified rendezvous is quite simple. We certify the free propagation of the chaser between each two impulses, thus obtain a certified enclosure of position and velocity before the next impulse, and finally update the velocity using the given value of the impulse. If time intervals under considerations are rather short, then we directly apply the validation method as in Section 3.1.3. On the contrary, for longer time intervals, techniques of Section 3.1.4 should be preferred.

We can lead further the analysis by taking interval values for impulses, modeling the fact that thrusters cannot be controlled with very high precision. This results in interval values for initial conditions after the impulse. Here, the use of a certified transition matrix instead of a straightforward application of the validation method with interval initial conditions is highly recommended, for in the former case the interval initial conditions will only appear at the end as they are multiplied by the transition matrix, whereas in the latter case, these interval values will intervene in the Newton-like operator and produce extremely overestimated error bounds.

Semi-major axis	6763 km
Eccentricity	0.0052
Initial time	$\nu_0 = 0$ rad.
Final time	$\nu_f = 8.1832$ rad.
Initial state	$(-30, 0.5, 8.514, 0)$ [km - m/s]
Final state	$(-100, 0, 0, 0)$ [m - m/s]

(a) Parameters of the mission

$\nu$	$\Delta\dot{x}$ [m/s]	$\Delta\dot{z}$ [m/s]
0.0	-7.50230589	0.742372034
1.388128	-1.55579123	0.08834686
6.666595	0.62565013	0.03325936
8.183058	1.06509710	0.11440204

(b) Impulses found by numerical algorithm

degree	$x(\nu_f)$	$z(\nu_f)$	$\dot{x}(\nu_f)$	$\dot{z}(\nu_f)$
25	-100 + [-2.6861e1, 2.6861e1]	[-7.4084e0, 7.4084e0]	[-1.8133e-2, 1.8133e-2]	[-5.3675e-3, 5.3675e-3]
30	-100 + [-1.0035e-1, 1.0035e-1]	[-2.7676e-2, 2.7676e-2]	[-6.7741e-5, 6.7741e-5]	[-2.0051e-5, 2.0051e-5]
40	-100 + [-2.3194e-5, 2.3190e-5]	[-6.3956e-6, 6.3956e-6]	[-1.5655e-8, 1.5655e-8]	[-4.6336e-9, 4.6336e-9]
50	-100 + [-2.0321e-8, 1.6320e-8]	[-5.0437e-9, 5.0607e-9]	[-1.2358e-11, 1.2376e-11]	[-3.6651e-12, 3.6555e-12]

(c) Final state, in function of the approximation degree. The brackets represent rigorously bounded uncertainties, e.g.  $-100+[-3e1,3e1]$  means a value between -130 and -70.**Figure 5:** A posteriori validation of ATV short rendezvous mission

## 4 Fuel optimal station keeping of a geostationary spacecraft equipped with a low-thrust propulsion system

For geostationary spacecraft station keeping control purposes, the non linear equations of motion can be linearized with respect to the station keeping point. In contrast to Tschauner-Hempel equations, the system is here coupled and will be hence a good illustration of the extension of the method presented in Section 2 to the vectorial case.

Section 4.1 introduces the model for the station keeping of a geostationary satellite with a low-thrust propulsion system and the linearization we will consider. Section 4.2 is still ongoing work and aims at providing certified polynomial transition matrices, which could later be used in optimal control algorithms.

### 4.1 Description of the model

**4.1.1 Minimum fuel non linear station keeping problem** The position and velocity of a satellite orbiting the Earth on a Geostationary Earth Orbit (GEO) is described with the equinoctial orbital elements as defined in [3]:

$$x_{eoe} = [a \ e_x \ e_y \ i_x \ i_y \ \ell_{M\Theta}]^T \in \mathbb{R}^6, \quad (22)$$

where  $a$  is the semi-major axis,  $(e_x, e_y)$  the eccentricity vector components,  $(i_x, i_y)$  the inclination vector components,  $\ell_{M\Theta} = \omega + \Omega + M - \Theta$  is the mean longitude where  $\Omega$  is the right ascension of the ascending node,  $\omega$  is the perigee's argument,  $M$  is the mean anomaly and  $\Theta(t)$  is the right ascension of the Greenwich meridian. The dynamics of the satellite may be represented by the follow-

ing non linear state-space model:

$$\frac{dx_{eoe}}{dt} = f_L(x_{eoe}, t) + f_G(x_{eoe}, t)u, \quad (23)$$

where  $f_L \in \mathbb{R}^6$  is the Lagrange contribution part of the external forces. As described in [32] or [31], the oblateness of the Earth gravitational potential, the third-body attraction of the Sun and the Moon, as well as the Sun Radiation Pressure (SRP) act as perturbations that make the spacecraft drift from its nominal position.

$f_G \in \mathbb{R}^{6 \times 3}$  is the Gauss contribution part.  $u = [u_R \ u_T \ u_N]^t \in \mathbb{R}^3$  is the control vector expressed in the local orbital  $RTN$  frame.

The geographical coordinates of the satellite:

$$y_{eoe} = T(x_{eoe}, t)x_{eoe}, \quad (24)$$

are of interest because the station keeping problem consists in constraining them in the vicinity of the station position  $y_{sk} = [r_{sk} \ 0 \ \lambda_{sk}]^t$  where  $r_{sk}$  is the synchronous radius and  $\lambda_{sk}$  is the station keeping geographical longitude. Denoting  $\delta$  the half width of the allowed station keeping window, the station keeping requirements read:

$$|\varphi| \leq \delta \text{ and } |\lambda - \lambda_{sk}| \leq \delta, \quad (25)$$

where  $\varphi$  and  $\lambda$  are respectively the geographic latitude and the geographic longitude of the spacecraft.

**4.1.2 Linearization** As the station keeping window size is very small with respect to the distance to the Earth, it is possible to linearize the non linear Equation 23. In order to express the station keeping problem, the relative state of the satellite with respect to the station keeping state is defined as:

$$x_{sk} = [a_{sk} \ 0 \ 0 \ 0 \ 0 \ \ell_{M\Theta_{sk}}]^t, \quad (26)$$

where  $a_{sk}$  is the synchronous semi-major axis and  $\ell_{M\Theta_{sk}}$  is the station mean longitude. This station keeping state is a fictitious point evolving on a keplerian (unperturbed) GEO orbit. It is defined such that the spacecraft mean motion equals the Earth rotation rate. It is then straightforward that :

$$\frac{dx_{sk}}{dt} = \left[ 0 \ 0 \ 0 \ 0 \ 0 \ \sqrt{\frac{\mu}{a_{sk}^3}} - \omega_T \right] = 0, \quad (27)$$

where  $\omega_T$  is the Earth rotation rate.

The relative dynamics equations are developed by linearization of Equation (23) about the station keeping point (26). By denoting  $x = x_{eoe} - x_{sk}$  the relative state model for the SK problem is computed as following:

$$\begin{aligned} \frac{dx}{dt} &= \frac{dx_{eoe}}{dt} - \frac{dx_{sk}}{dt}, \\ &= f_L(x_{eoe}, t) + f_G(x_{eoe}, t)u - 0, \\ &\approx f_L(x_{sk}, t) + \left. \frac{\partial f_L(x_{eoe}, t)}{\partial x_{eoe}} \right|_{x_{eoe}=x_{sk}} x + f_G(x_{sk}, t)u, \end{aligned} \quad (28)$$

assuming that the product of the state vector and the control vector components are of order 2. The computations of Equation (28) allows to described the motion of a geostationary satellite as the relative motion with respect with a fictitious point evolving on a keplerian GEO orbit and the dynamical model reads:

$$\frac{dx}{dt} = A(t)x + D(t) + B(t)u, \quad (29)$$

where the matrices  $A \in \mathbb{R}^{6 \times 6}$ ,  $B \in \mathbb{R}^{6 \times 3}$ ,  $C \in \mathbb{R}^{3 \times 6}$  and  $D \in \mathbb{R}^6$  are defined as follows:

$$A(t) = \left. \frac{\partial (f_L(x_{eoe}(t), t))}{\partial x_{eoe}} \right|_{x_{eoe}=x_{sk}}, \quad (30)$$

$$B(t) = f_G(x_{sk}, t), \quad (31)$$

$$D(t) = f_L(x_{sk}, t), \quad (32)$$

The relative geographical position with respect to the station-keeping position is denoted by:

$$y = y_{eoe} - y_{sk} = T(x_{sk}, t)x = C(t)x, \quad (33)$$

and is obtained by linearizing Equation (24).

After the linearization, the station keeping requirements on the latitude and the longitude of the spacecraft are expressed in terms of the state vector as:

$$|[0 \ 1 \ 0]C(t)x(t)| \leq \delta \text{ and } |[0 \ 0 \ 1]C(t)x(t)| \leq \delta \ \forall t \in [0, T], \quad (34)$$

The linear GEO station keeping control problem is expressed as the following optimal control problem:

$$\begin{aligned} & \min_u \int_{t_0}^{t_f} \|u(t)\|_1 dt, \\ \text{s.t. } & \begin{cases} \dot{x}(t) = A(t)x(t) + D(t) + B(t)u(t), \\ x(t_0) = x_0, \\ |[0 \ 1 \ 0]C(t)x(t)| \leq \delta, \\ |[0 \ 0 \ 1]C(t)x(t)| \leq \delta, \end{cases} \end{aligned} \quad (35)$$

where  $t_0$  is the initial time,  $t_f$  is the station keeping horizon and  $x_0$  is the initial state vector.

The reference [17] or [4] describe how the direct collocation methods can be used in order to solve the optimal control problem. These methods rely on a discretization of the state and control vectors over the time interval  $[t_i, t_f]$ , with  $t_i$  the initial time and  $t_f$  the final time. The optimal control problem is therefore transformed into a non linear programming problem.

The dimension of the unknown vector for the non linear programming problem can be reduced while eliminating the state vector, meaning that the state differential equation of the system must be integrated explicitly. In the reference [13], the linear time varying system for the geostationary station keeping problem is approximated assuming that the matrices are constant on each subinterval of the discretization, and an approximate state transition matrix can be computed.

The method proposed in Section 2 aims at using Chebyshev polynomials to compute the state transition matrix. Doing so, the error made while integrating the state dynamics can be estimated, and the time mesh can be well adjusted.

Another method for solving the minimum fuel station keeping problem described in [12] can be improved by using the proposed state transition matrices integration method. In order to optimize the commutation times of a bang-bang control profile, the state dynamics and the derivative of the state dynamics with respect to the commutation times have to be numerically integrated, what can lead to long computation times in the case where the control profile commutes frequently. The integration time could be reduced with the polynomial based computation of the state transition matrix.

In order to express the relative GEO station keeping linear dynamical model, the external perturbations have to be linearized. A first example is computed for which only the so-called J2 perturbation is taken into account.

**4.1.3 Geostationary station keeping with the J2 perturbation** The only perturbation taken into account in this simple example is the J2 term of the Legendre decomposition of the Earth potential. The potential is given by (see [9]):

$$\mathcal{E} = \frac{\alpha}{r^3} \left( \frac{3}{2} \sin^2 \varphi - \frac{1}{2} \right), \quad (36)$$

where  $r$  is the radius,  $\varphi$  is the geographical latitude and  $\alpha = -\mu R_T^2 J_2$ . Applying the Lagrange perturbation theory expressed with the equinoctial orbital elements (see [3]), the expression of the function  $f_L(x_{eoe}, t)$  from Equation (23) can be found in [23].

Performing the linearization with respect to the fictitious point evolving on a keplerian geostationary orbit as proposed in the previous paragraph, the

linearized dynamical model reads:

$$A(t) = \begin{bmatrix} 0 & \frac{3\alpha \sin \phi_s(t)}{a_s^2 \sqrt{\mu a_s}} & -\frac{3\alpha \cos \phi_s(t)}{a_s^2 \sqrt{\mu a_s}} \\ -\frac{21\alpha \sin \phi_s(t)}{4a_s^4 \sqrt{\mu a_s}} & \frac{6\alpha \cos \phi_s(t) \sin \phi_s(t)}{a_s^3 \sqrt{\mu a_s}} & \frac{6\alpha \sin^2 \phi_s(t)}{a_s^3 \sqrt{\mu a_s}} \\ \frac{21\alpha \cos \phi_s(t)}{4a_s^4 \sqrt{\mu a_s}} & -\frac{6\alpha \cos^2 \phi_s(t)}{a_s^3 \sqrt{\mu a_s}} & -\frac{6\alpha \cos \phi_s(t) \sin \phi_s(t)}{a_s^3 \sqrt{\mu a_s}} \\ 0 & 0 & 0 \\ 0 & 0 & 0 \\ -\frac{3}{2} \sqrt{\frac{\mu}{a_s^5}} + \frac{21\alpha \sin \phi_s(t)}{2a_s^4 \sqrt{\mu a_s}} & \frac{39\alpha \cos \phi_s(t)}{a_s^3 \sqrt{\mu a_s}} & -\frac{39\alpha \sin \phi_s(t)}{4a_s^3 \sqrt{\mu a_s}} \\ 0 & 0 & \frac{3\alpha \cos \phi_s(t)}{2a_s^3 \sqrt{\mu a_s}} \\ 0 & 0 & 0 \\ 0 & \frac{3\alpha \sin \phi_s(t)}{2a_s^3 \sqrt{\mu a_s}} & 0 \\ \frac{3\alpha \cos \phi_s(t) \sin \phi_s(t)}{a_s^3 \sqrt{\mu a_s}} & -\frac{3\alpha \cos^2 \phi_s(t)}{a_s^3 \sqrt{\mu a_s}} & 0 \\ \frac{3\alpha \sin^2 \phi_s(t)}{a_s^3 \sqrt{\mu a_s}} & -\frac{3\alpha \cos \phi_s(t) \sin \phi_s(t)}{a_s^2 \sqrt{\mu a_s}} & 0 \\ 0 & 0 & 0 \end{bmatrix}, \quad (37)$$

and

$$D(t) = \begin{bmatrix} 0 \\ \frac{3\alpha \sin \phi_s(t)}{2a_s^3 \sqrt{\mu a_s}} \\ \frac{3\alpha \cos \phi_s(t)}{2a_s^3 \sqrt{\mu a_s}} \\ 0 \\ 0 \\ \frac{-3\alpha}{a_s^3 \sqrt{\mu a_s}} + \sqrt{\frac{\mu}{a_s^3}} - \omega_T \end{bmatrix}, \quad (38)$$

where  $\phi_s(t) = \ell_{M\Theta,sk} + \Theta(t)$

## 4.2 Certified semi-analytical transition matrices for geostationary model

This section is still on-going work, but all the computations, with different parameters, shall be soon available.

**4.2.1 Approximating Chebyshev expansion** For the moment, we only had time to perform a single computation to obtain a Chebyshev approximation of degree 250 of the relative motion over 20 days. Results for the six components are given in Figure 6.

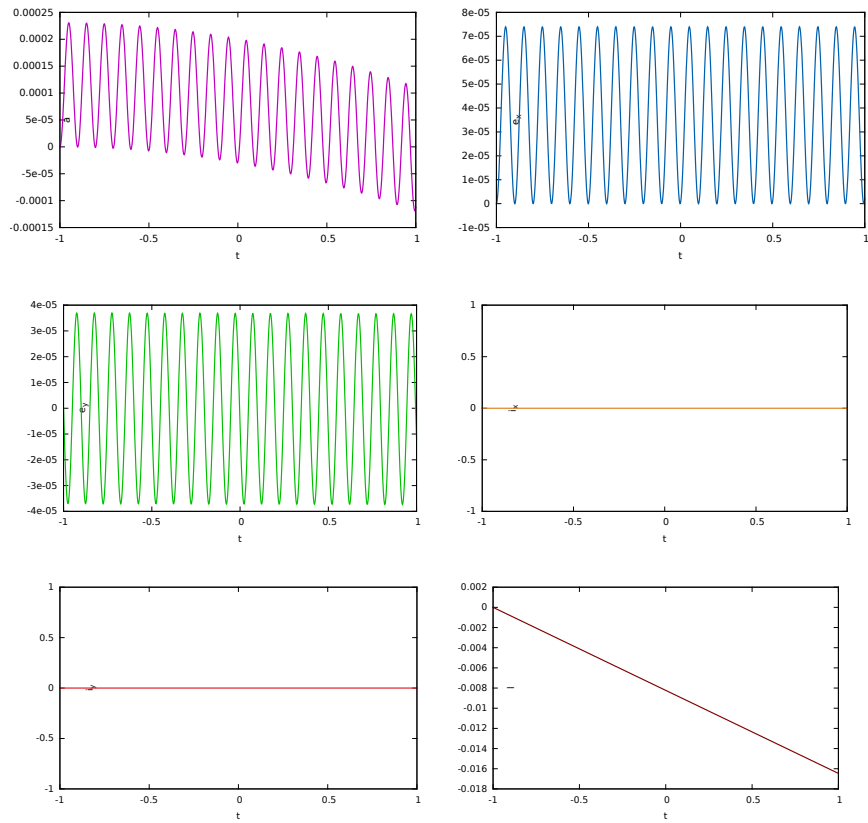


**Figure 6:** Numerical Chebyshev approximation for geostationary trajectory propagation with J2 perturbation

**4.2.2 Validated transition matrices** The same techniques for long-term propagation as in Section 3.1.4 can be used, so that a contracting operator can be computed for only one period. Concrete validation examples will be carried out soon.

## 5 Conclusion and future developments

The first short term objective is to test our semi-analytical transition matrices for several optimal control problems, like spacecraft rendezvous and geostationary station keeping with several perturbations such as Earth oblateness, solar and lunar attraction, atmospheric drag and solar radiation pressure. Focusing on the design of on-the-fly autonomous control laws, we foresee embedding this method on a board dedicated to space applications, evaluate the execution times and assess the trade-off between precision and computational burden.

A second short term objective is to propose several examples of propagation of uncertain initial conditions via our semi-analytical polynomial transition matrix. When the uncertainties in the initial conditions are not uniformly distributed, we plan consider the generalization to other classes of orthogonal polynomials, like Legendre polynomials, or Hermite polynomials. In fact, orthogonal polynomials always satisfy a three-term-recurrence, so that the multiplication and integration formulas remain similar, which should produce similar almost-banded integral operators. Finally, we investigate the generalization of our method to nonlinear dynamics, based on similar Newton-like iteration methods.

## Acknowledgements

This work was supported by the FastRelax (ANR-14-CE25-0018-01) project of the French National Agency for Research (ANR), by the French Space Agency (CNES) and Thales Alenia Space.

## References

- [1] P. R. Arantes Gilz, M. Joldes, C. Louembet, and F. Camps. Model predictive control for rendezvous hovering phases based on a novel description of constrained trajectories. In *IFAC 2017 World Congress, Toulouse, to appear*, July 2017.
- [2] P. R. Arantes Gilz and C. Louembet. Predictive control algorithm for spacecraft rendezvous hovering phases. In *Control Conference (ECC), 2015 European*, pages 2085–2090. IEEE, 2015.
- [3] R. H. Battin. *An Introduction to the Mathematics and Methods of Astrodynamics*. Education. AIAA., 1999.
- [4] J. T. Betts. Survey of numerical methods for trajectory optimization. *Journal of Guidance, Control, and Dynamics*, 21(2):193–207, 1998.
- [5] J. P. Boyd. *Chebyshev and Fourier spectral methods*. Dover Publications, 2001.

- [6] F. Bréhard, N. Brisebarre, and M. Joldes. Validated and numerically efficient Chebyshev spectral methods for linear ordinary differential equations. Preprint, May 2017.
- [7] G. Campan and P. Brousse. ORANGE: Orbital analytical model for geosynchronous satellite. *Revista Brasileira de Ciências Mecânicas (ISSN 0100-7386)*, vol. 16, p. 561-572, 16:561–572, 1994.
- [8] M. Claeys, D. Arzelier, D. Henrion, and J.-B. Lasserre. Moment LMI approach to LTV impulsive control. In *Decision and Control (CDC), 2013 IEEE 52nd Annual Conference on*, pages 5810–5815. IEEE, 2013.
- [9] CNES. *Mécanique Spatiale, Tome II*. Toulouse, France, Cepadues-E edition, 1995.
- [10] G. Deaconu, C. Louembet, and A. Theron. Constrained periodic spacecraft relative motion using non-negative polynomials. In *American Control Conference (ACC), 2012*, pages 6715–6720. IEEE, 2012.
- [11] G. Di Mauro, M. Schlotterer, S. Theil, and M. Lavagna. Nonlinear control for proximity operations based on differential algebra. *Journal of Guidance, Control, and Dynamics*, 38(11):2173–2187, 2015.
- [12] C. Gazzino, D. Arzelier, L. Cerri, D. Losa, C. Louembet, and C. Pittet. A minimum-fuel fixed-time low-thrust rendezvous solved with the switching systems theory. 2017.
- [13] C. Gazzino, C. Louembet, D. Arzelier, N. Jozefowicz, D. Losa, C. Pittet, and L. Cerri. Integer programming for optimal control of geostationary station keeping of low-thrust satellites. 2017.
- [14] D.-W. Gim and K. T. Alfriend. State transition matrix of relative motion for the perturbed noncircular reference orbit. *Journal of Guidance, Control, and Dynamics*, 26(6):956–971, 2003.
- [15] D. Gottlieb and S. A. Orszag. *Numerical Analysis of Spectral Methods: Theory and Applications*, volume 26. Siam, 1977.
- [16] E. N. Hartley. A tutorial on model predictive control for spacecraft rendezvous. In *Control Conference (ECC), 2015 European*, pages 1355–1361. IEEE, 2015.
- [17] D. G. Hull. Conversion of optimal control problems into parameter optimization problems. *Journal of Guidance, Control, and Dynamics*, 20(1):57–60, 1997.
- [18] A. Iserles. *A first course in the numerical analysis of differential equations*. Number 44. Cambridge University Press, 2009.
- [19] J.-B. Lasserre. *Moments, positive polynomials and their applications*, volume 1. World Scientific, 2009.
- [20] J.-P. Lessard and C. Reinhardt. Rigorous numerics for nonlinear differential equations using Chebyshev series. *SIAM Journal on Numerical Analysis*, 52(1):1–22, 2014.

- [21] P. D. Lizia, R. Armellin, and M. Lavagna. Application of high order expansions of two-point boundary value problems to astrodynamics. *Celestial Mechanics and Dynamical Astronomy*, 102(4):355–375, 2008.
- [22] P. D. Lizia, R. Armellin, A. Morselli, and F. Bernelli-Zazzera. High order optimal feedback control of space trajectories with bounded control. *Acta Astronautica*, 94(1):383 – 394, 2014.
- [23] D. Losa. *High vs low thrust station keeping maneuver planning for geostationary satellites*. PhD thesis, École Nationale des Mines de Paris, 2007.
- [24] J. C. Mason and D. C. Handscomb. *Chebyshev polynomials*. CRC Press, 2002.
- [25] Y. Nesterov. Squared functional systems and optimization problems. In *High performance optimization*, pages 405–440. Springer, 2000.
- [26] S. Olver and A. Townsend. A fast and well-conditioned spectral method. *SIAM Review*, 55(3):462–489, 2013.
- [27] J. B. Rawlings and D. Q. Mayne. *Model predictive control: Theory and design*. Nob Hill Pub., 2009.
- [28] A. Riccardi, C. Tardioli, and M. Vasile. *An intrusive approach to uncertainty propagation in orbital mechanics based on Tchebycheff polynomial algebra*, pages 707–722. Advances in Astronautical Sciences, AAS/AIAA Astrodynamics Specialist Conference, August 9-13, 2015, Vail, Colorado, U.S.A. American Astronautical Society, 8 2015.
- [29] I. M. Ross. 6 - Space Trajectory Optimization and L1-Optimal Control Problems. In P. Gurfil, editor, *Modern Astrodynamics*, volume 1 of *Elsevier Astrodynamics Series*, pages 155 – 188. Butterworth-Heinemann, 2006.
- [30] H. Schaub. Relative orbit geometry through classical orbit element differences. *Journal of Guidance, Control, and Dynamics*, 27(5):839–848, 2004.
- [31] M. J. Sidi. *Spacecraft Dynamics and Control*. Cambridge University Press, 1997.
- [32] E. M. Soop. *Handbook of Geostationary Orbits*. Kluwer Academic Publishers Group, 1994.
- [33] J. Tschauner and P. Hempel. Optimale beschleunigungsprogramme fur das rendezvous-manoever. *Astronautica Acta*, 10(5-6):296–+, 1964.
- [34] N. Yamamoto. A numerical verification method for solutions of boundary value problems with local uniqueness by Banach’s fixed-point theorem. *SIAM Journal on Numerical Analysis*, 35(5):2004–2013, 1998.
- [35] K. Yamanaka and F. Ankersen. New state transition matrix for relative motion on an arbitrary elliptical orbit. *Journal of Guidance, Control, and Dynamics*, 25(1):60–66, 2002.